Journal of Applied Polymer Science

A morphological study on the migration and selective localization of graphene in the PLA/PMMA blends

Azin Paydayesh,[1] Ahmad Arefazar,[1,2] Azam Jalaliarani[1,2]
[1]AmirKabir University of Technology, Mahshahr Campus, Mahshahr, I.R. Iran
[2]Polymer Engineering Department, Amir Kabir University of Technology, Tehran, I.R. Iran
Correspondence to: A. Arefazar (E-mail: arefazar@aut.ac.ir)

ABSTRACT: Nano-filled polymer blends offer the opportunity to obtain materials with fine-tuned properties. In this work, the dispersion and localization behavior of graphene nanoplate (GNP) and graphene oxide (GO) in solution mixed blends of polylactic acid (PLA) and polymethyl methacrylate (PMMA) were investigated. The blends were prepared by using different mixing sequences to investigate the effect of kinetics parameters and surface chemistry of filler as well as thermodynamics affinity on the localization of fillers. Field Emission Scanning Electron Microscopy (FESEM) and Rheometric Mechanical Spectroscopy (RMS) were employed. In addition, graphene materials were compared by Fourier transform infrared and Raman spectroscopy as well as elemental analysis characterization. Results showed that depending on the mixing sequence, the GNPs were localized in the both phases and interface through migration to reach thermodynamics equilibrium. However, GO localization was significantly affected by the mixing sequence due to better interaction with the polymer phases. © 2016 Wiley Periodicals, Inc. J. Appl. Polym. Sci. **2016**, *133*, 43799.

KEYWORDS: graphene; morphology; polymer blend; rheology; selective localization

Received 9 December 2015; accepted 17 April 2016
DOI: 10.1002/app.43799

INTRODUCTION

One of the conventional methods used to improve the properties of polymeric materials is the blending of polymers. Polymer blends constitutes a large proportion of the materials used in polymer production and are still increasing in demand at a level that is far above average.[1]

In recent years, incorporation of nano-fillers into immiscible polymer blends has received tremendous attention.[2–4]

It is a well-known fact that the properties of filled polymers depends strongly on the arrangement of the filler in the polymer. This factor is very important in filled immiscible polymer blends. Therefore, control of filler dispersion and filler distribution in the polymer blend is essential in the generation of materials with desirable properties.

When a nano-filler is added to an immiscible polymer blend, fillers may be located either at the polymer phases or at the interphase. The position of the filler is predicted by classical thermodynamics. Preferential filler localization is commonly explained by the differences in interfacial energies between fillers and polymer phases, which determine the ability of the filler to be wetted by the respective polymers.[5,6] Filler is adsorbed by the phase with minimum interfacial tension.

Conventionally, Young's equation is used in the prediction (estimation) of filler localization in polymer blends that are in equilibrium state according to the wetting coefficient(or contact angle) calculation[7]:

$$\cos\theta = \omega_a = \frac{\gamma_{s-1} - \gamma_{s-2}}{\gamma_{2-1}} \quad (1)$$

Where θ is contact angle, ω_a is the wetting coefficient, $\gamma_{s\text{-}1}$ and $\gamma_{s\text{-}2}$ are the interfacial energies between the solid filler and polymer phases and $\gamma_{2\text{-}1}$ is the interfacial energy between the respective polymers. According to the ω_a, three cases are possible:

-$\omega_a < -1$,filler preferentially located within polymer 1
-$\omega_a > 1$, filler preferentially located within polymer 2
-$1 < \omega_a < -1$, filler preferentially located at the interface of the polymer blend

To obtain the wetting coefficient, the values of interfacial tensions of the filler and polymer phases are required. They can be calculated from surface energies as well as their polar and disperse parts with the aid of models like Grifalco-Good,[8,9] Owen-Wendt (commonly known as geometric mean)[10,11] and Wu model (commonly known as harmonic mean)[6,12] equations [eqs. (2–4)]:

$$\gamma_{12} = \gamma_1 + \gamma_2 - 2\sqrt{\gamma_1\gamma_2} \quad (2)$$

$$\gamma_{12}=\gamma_1+\gamma_2-2\sqrt{\gamma_1^d\gamma_2^d}-\sqrt{\gamma_1^p\gamma_2^p} \quad (3)$$

$$\gamma_{12}=\gamma_1+\ \gamma_2\ -4\left(\frac{\gamma_1^d\gamma_2^d}{\gamma_1^d+\gamma_2^d}+\frac{\gamma_1^p\gamma_2^p}{\gamma_1^p+\gamma_2^p}\right) \quad (4)$$

Where γ_1 and γ_2 are the surface energies of component 1 and 2, γ_1^p, γ_2^p, γ_1^d and γ_2^d are the polar parts and disperse parts of the surface energies of component 1 and 2 respectively.

In research literatures, geometric mean is considered more suitable for high surface energy materials while the harmonic mean is considered more suitable for low surface energy materials.[13]

Fenouillot and co-workers reviewed works on wetting parameter and filler localization in several cases.[5] Although the filler localization has been estimated correctly in many studies, in a number of studies, there have been discrepancies between the theoretical predictions and experimental observations. These results suggest that the knowledge of wetting coefficient is not sufficient to determine the arrangement of filler in a polymer blend.

It should be noted that particle localization agreement with the thermodynamics of wetting only prove the thermodynamic equilibrium achievement.[5] Thus, the kinetics effects can influence the filler position and should be considered carefully.

One of the most important factors involved in the dispersion of filler and its distribution in the polymer blend is the processing condition. The order of addition of components has a strong effect on the kinetics. This factor has been investigated in several cases,[6,14–16] often in melt-mixing process. Usually, different mixing sequences are considered in investigating the conflict between thermodynamic control and kinetics control in order to attain a final morphology. Depending on the selected sequence, the affinity of the filler to the phases and the processing time, different scenarios are possible. Sometimes, filler transfer could be to the preferred phase or to the interface for it to reach equilibrium distribution. Elias *et al.*, has proposed and discussed the migration mechanism of filler in the blend from one phase to the other.[17] In another research, Godlel *et al.* showed that the opportunity for migration of filler depends on the time of mixing and the aspect ratio of filler. It seems as though fillers with low aspect ratio can be transferred much easier than fillers with high aspect ratio.[18,19]

In addition, the effect of viscosity ratio of polymer phases on the localization and migration ability of filler was investigated and discussed in literatures.[20–22] Based on these papers, analysis of viscosity effect is difficult and sometimes exhibit discrepancies because of local and temporal variation in viscosity during mixing.

There are some papers that compared filler localization predicted by wetting coefficient and experimental observation in an immiscible polymer blend.[23–28]

However, the knowledge on localization of graphene nanoplates' polymer blends is still insufficient.

Based on our knowledge, up to this moment, only Liebscher *et al.*, has studied the selective localization of graphene in PC/SAN blend by varying the mixing sequence and mixing parameters in melt-mixed process.[29] They reported different dispersion states and different filler localization due to variation in mixing conditions but in all samples, the dispersion of graphene nanoplates (GNPs) was very poor and involved large agglomerations. However, the localization of GNPs in immiscible polymer blend has never been discussed in literatures on solution blending.

The aim of this study was to investigate the localization of high aspect ratio filler such as graphene and the possibility of its transfer between the phases in an immiscible polymer blend during solution mixing. In addition, the effect of filler surface chemistry on selection location of filler was examined.

In research literatures, often, a blend of two polymers with significant difference in polarity has been selected, and migration and localization of filler have been investigated. However, in this work, the polylactic acid (PLA)/polymethyl methacrylate (PMMA) polymer blend with similar polarity was selected to manipulate the conflict between kinetics parameters and thermodynamics.

EXPERIMENTAL

Material

Poly(lactic acid) with a melt flow rate of 6 g/10 min and $M_w = 246{,}500$ g/mol, (PLA, 2003D) was supplied by Nature Works LLC.

PMMA used in this study was obtained from Chimei Co. (Agryrex 205), with a melt flow index of 1.8 g/10 min and $M_w = 90{,}400$ g/mol. GNPs and graphene oxide nanoplates (GO) were purchased from Graphene Expert Co. Based on data obtained from the company, the average thickness of GNP and GO is approximately 7–10 layers and <3 layers respectively.

Prior to processing, PLA and PMMA were dried in an oven at 90 °C for 4 hours to remove residual moisture, and thereafter stored in a desiccator before usage.

Chloroform and DMF, which are the solvent used in this experiment were purchased from Daejung Co. and used as received from the company.

Sample Preparation Procedure

PLA/PMMA/GNPs and PLA/PMMA/GO nanocomposites were prepared by solution-mixing blending. Firstly, GNPs (or GO) was dispersed in chloroform by stirring for one day and the sonication was done for 30 min at room temperature. Then, the graphene suspension was combined with the polymer phases using four different procedures:

Direct blending of all components in one processing step. In this procedure, polymer components and graphene suspension were combined together simultaneously and stirred overnight (named as S-1-G and S-1-GO for GNP filled blends and GO filled blends respectively).

This procedure involves blending predominant amounts of PLA with PMMA and then adding GNPs suspension. In this way, the blend of PLA/PMMA was formed and graphene (or GO) was thereafter introduced into the blend (named as S-2-G and S-2-GO). This compound was stirred overnight.c, d)the third

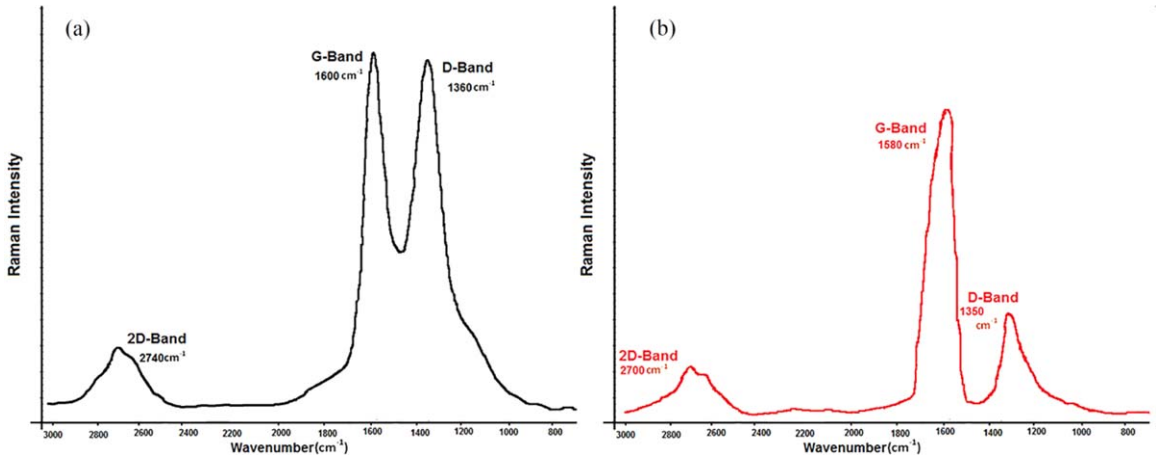

Figure 1. The Raman spectra of GNP and GO. [Color figure can be viewed in the online issue, which is available at wileyonlinelibrary.com.]

and fourth procedures involves the preparation of premixed PLA-GNPs (S-3-G and S-3-GO) or premixed PMMA-GNPs (as S-4-G and S-4-GO respectively) by stirring for one day, and combination of the premix with the other respective unfilled polymers. These compounds were stirred for another day.

All samples contained 40 wt % PLA, 60 wt % PMMA and GNPs (or GO) concentration of 0.5 phr Samples were casted in Petri dish and dried at ambient temperature for 24 h.

Characterization

Raman. Raman spectroscopy was performed using First Guard, Rigarku, USA to characterize the structural parameters of graphene and GO in 600–3000 cm^{-1} range with a laser excitation wavelength of 532 nm and a laser power of 0.1 mw.

Elemental Analysis. Elemental analysis by combustion was performed by an EA1110-FISONS (Thermo Quest Italia S.P.A, Italy) and with a Flash EA1112 (Thermo Finnigan, Italy) for Carbon, Hydrogen, Nitrogen and Oxygen elements respectively.

FTIR. Fourier transform infrared (FTIR) spectroscopy spectra were measured with a Nicolet Nexus-870 spectrometer (Madison, WI) that had an attenuated total reflectance (ATR) technique in the region of 400–4000 cm^{-1}. The average often scans was computed for each sample.

FESEM. The morphology and GNPs and GO dispersion as well as localization in the polymer blend was observed using a field emission scanning electron microscope (FESEM) Mira 3-XMU with a 20 Kv acceleration voltage. To obtain the phase morphology of the blends, samples were cryo-fractured in liquid nitrogen. Thereafter, the fractured surface was etched in DMF at room temperature for 1h for it to be selectively dissolved in the PMMA phase. The etched surface was coated with a gold layer before SEM characterization.

TEM. In order to evaluation and comparison between the dispersion state of two graphene based materials, TEM measurements were conducted on a Tecnai 20 (FEI Corp., USA) transmission electron microscopy operated at an acceleration voltage of 200 kV. Samples were cut to ultrathin films at room temperature by a microtome (LEICA ULTRACUTR ME1-057) equipped with a glass knife.

RMS. The linear viscoelastic behavior of all the samples was measured using Rheometric Mechanical Spectrometry. The oscillatory shear measurements were performed at 220 °C under nitrogen atmosphere to prevent polymer degradation using MCR301 rheometer (Physica Anton Paar, Austria) fitted with a 25 mm parallel plate geometry and a gap of 1 mm. The frequency sweep experiment was carried out by monitoring storage modulus over a frequency range of 0.1∼100 rad/s in small strain oscillatory shear deformations in order to determine linear viscoelastic behavior.

RESULTS AND DISCUSSION

Graphene and Graphene Oxide Characterization

The Raman spectra of GNP and GO are shown in Figure 1. Graphenic materials exhibit a relatively simple Raman spectrum with three characteristic vibration bands designed as the G band(the tangential mode for sp^3 hybridized carbons), D band (disorder mode for sp^2 hybridized carbons) and 2D band (the second order of D band). By analyzing the intensity, shape and band's peak position, the vital information on graphene structure and its layer thickness can be obtained. The number of layers can be seen from the ratio of peak intensity of the 2D band to the G band as well as the position and shape of these peaks.[30,31]

The Raman spectrum of GNP [Figure 1(a)] shows an intensive G band at 1580 cm^{-1} and a less intensive D band at 1350cm^{-1} and 2D band at 2700 cm^{-1} with a shoulder at 2610 cm^{-1}. This spectrum exhibited graphite like structure with many layers for GNP. But the for GO [Figure 1(b)] G band is at 1600 cm^{-1}, D band at 1360 $cm^{-1}$and the 2D band at 2740 cm^{-1}. In this case, the I_{2D}/I_G increased approximately by 20% indicating a partial exfoliation of GNP. Thus, GO contains lower layer numbers in comparison with GNP.

FTIR spectroscopy was used to identify chemical structure, i.e functional groups of GNP and GO, as shown in Figure 2.For GNP [Figure 2(a)] the absorption peaks appear at 3600 cm^{-1} (O—H free), at 2750 cm^{-1} (stretching vibrations of CHO from aldehyde), at 1700 cm^{-1} (stretching vibrations from C═O), at 1540 cm^{-1} (C═C stretching vibrations of aromatic structure), and at 1051 cm^{-1} (C—O stretching vibrations). In the spectrum

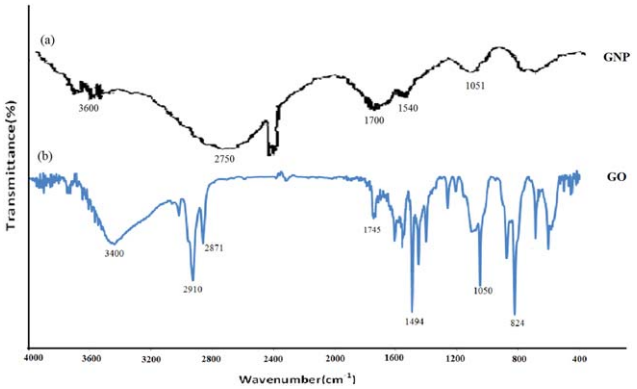

Figure 2. FTIR spectra of GNP and GO. [Color figure can be viewed in the online issue, which is available at wileyonlinelibrary.com.]

of GO [Figure 2(b)], the absorption peaks appear at 3400 (O—H free), at 2910, 2871 cm^{-1} (C—H stretching vibrations), at 1754 cm^{-1} (stretching vibrations from C═O) and C═C stretching vibrations at 1540 cm^{-1}. The absorption peaks at 824, 854 and 1050 cm^{-1} that is attributed to the epoxy group.

Since graphene is obtained from the chemical reduction of GO (based on supplier information), small amounts of oxygen containing groups were remained on the graphene in this research. Thus, there are some types of oxygen functionalities on both nano sheets.

To investigate the degree of reduction of GNPs, elemental analysis was performed. As shown in Table I, the C/O ratio of GO was ≈2.5 while that GNP was ≈8.5 indicating that a lot of oxygen atoms were removed by the chemical reduction and there were only a little amount of oxygen containing groups on the GNP. The presence of S and N components in the samples is due to oxidation by H_2SO_4 and reduction of GO by hydrazine (NH_2NH_2).

Filler Localization Prediction

The localization of GNP and GO within immiscible PLA/PMMA blend was predicted by calculation of the wetting coefficient ω_a as given by eq. (1). Table II list the surface energies for PLA, PMMA, GNP and GO obtained from literature.

Interfacial tension between the different blend components using surface energies was determined using the Grifalco-Good model, geometric and harmonic mean equations [eqs. (2–4)] and is presented in Table III.

Table I. Elemental Analysis of GNP and GO

	C (wt %)	H (wt %)	O (wt %)	N (wt %)	S (wt %)	C/O[a]
GNP	81.54	0.94	12.68	<0.5	0.715	2.44
GO	47.16	2.32	40.57	<0.5	1.2	8.57

[a] Corrected for water content.

Table II. The Surface Tension of the Blend Components

	γ^p (mJ/m^2)	γ^d (mJ/m^2)	γ (mJ/m^2)	Ref.
PLA	17.3	17.5	34.8	32
PMMA	11.55	29.55	41.1	33,34
GNP	13.2	41.6	54.8	35-37
GO	30	32.1	62.1	35

From the values of interfacial tension, the wetting coefficient values were calculated and fillers localization was estimated, which are presented in Table IV.

According to geometric and harmonic mean equations, thermodynamics predicted that the GNP located within the PMMA phase and GO should be localized at the interface of polymers. However, the Grifalco-Good equation predicted the localization of both GNP and GO in the PMMA phase. However, due to more accuracy of the geometric and harmonic mean equation, arising from the dispersive and polar parts of surface energies of the components, these equations were more reliable and more applied in the literature.

However, these models were proposed based on the thermodynamic affinity of filler, and the kinetics effects like viscosity ratio of the phases, sequence of mixing etc were disregarded.

Effect of Various Sequences on Filler Localization

The morphology of blends and the extent of GNP and GO dispersion and localization were investigated using FESEM. Each blend was prepared with a different sequence of filler incorporation, but with similar weight and phase composition of 40 wt % PLA, 60 wt %. PMMA and 0.5 phr of GNP or GO. In all the samples, the PMMA phase was etched using DMF. Thus, the dark and empty areas showed the PMMA phase.

FESEM Observation of GNP Localization. Figures 3–6 show the FESEM photographs of PLA/PMMA/GNP under different magnification for better observation. All blends showed sea-island morphology. In these samples, the PMMA phase formed the dispersed domains while the PLA formed the continuous matrix phase. In these images, the PMMA domain size and shapes are different. Considering composition similarity of all blends, the difference indicated the effect of processing condition, which may be different from the localization of filler in the first instance.

Figures 3 and 4 show the S-1-G (simultaneous mixing of three components) and S-2-G (first premixed of blend and then GNP mixing) samples. The average diameter of PMMA domains allowed for statistical variations was almost similar in both (about 2–10 μm). Some small aggregates of GNP are present in the PLA matrix phase in both samples and the presence of GNP in the interface is clear in Figures 3(a) and 4(a). However, the amount of GNP in the S-1-G blend was very low. It seems as though some of the GNPs located in the PMMA that were etched with PMMA were accorded experimental observation during etching. In addition, it is well known that the localization of filler in the dispersed phase in the case of polymer blends; make the dispersed droplets larger and more stable, thus the existence of

Table III. The Interfacial Tension between of the Phases of Blend

Materials	Interfacial energy (mJ/m^2) (Grifalco-Good model)	Interfacial energy (mJ/m^2) (Owen-Wendt model)	Interfacial energy (mJ/m^2) (Wu model)
PLA/PMMA	0.27	2.149	4.23
PLA/GNP	2.27	5.42	10.41
PMMA/GNP	0.99	1.01	2.18
PLA/GO	3.92	4.21	7.72
PMMA/GO	2.16	4.39	8.32

some larger PMMA domains would likely uphold the localization of GNP aggregates into the droplets.

However, the presence of GNP in the matrix of S-2-G sample was more observed than in S-1-G and the size and shape of PMMA domains was more homogenous. It seems as though the localization of larger amounts of GNP in the matrix prevented coalescence of droplets and produced more uniform morphology.

In fact, the observation from both samples was in contrast with the thermodynamic predictions. In these samples, the major amounts of GNP were located in the PMMA phase, not all of them. Localization of filler in the case of S-2-G was more complex. In this case, the morphology of the blend was formed first and thereafter GNP was introduced into the blend. Thus, GNP must pass through the PLA matrix for it to be localized in the preferred PMMA phase, but some of them were caught in the PLA matrix. As demonstrated in our previous papers,[38,39] (by FTIR, mechanical and thermal behavior of blend) GNP has interaction with both polymer phases but its affinity and interaction with PMMA phase is more than that for PLA phase. Therefore, Young equation predicted the localization of GNP in the PMMA.

When GNP was first premixed with PLA (S-3-G), although some small aggregates of GNP were observed in the PLA phase, however, most of them migrated to the PMMA phase, which is mainly located in this phase; see Figure 5(a–d). In addition, some of them were stuck in the interface during migration, which could easily be recognized especially in Figure 5(d).

When GNP was first premixed with PMMA (the preferred phase) and then mixed with PLA phase (lower affinity phase), the GNP were mainly located in the PMMA phase, which confirm the thermodynamics prediction, see Figure 6(a–d)

In all images of this sample, the size of PMMA domains were larger than that of the other samples and were more homogenous (compare with Figures 3–5) resulting in localization of GNP in this phase as mentioned before.

FESEM Observation of GO Localization. The morphology of GO containing blends is shown in Figures 7–10. By comparing the GNP filled blends with GO filled blends, it was obvious that in all the GO containing samples, morphology became finer and more uniform indicating the compatibilizing effect of GO in these blends. It should be noted that as shown and explained in the previous section ("FESEM Observation of GNP Localization" section), GO has more polar and functional groups than GNP and thus has more interaction and compatibility with the polar PLA and PMMA polymers. The aggregates of GNP were obvious in the GNP filled blends but the aggregates of GO were smaller with lower layers and fully exfoliated [see Figure 7(d)] in the blends.

In the simultaneously mixed sample (S-1-GO), the GO was observed in both polymeric phases and in the interface [see Figure 7(b)]. When the blend was premixed and then GO added, (S-2-GO), the morphology became completely fine and homogenous as shown in Figure 8(a–d). It seems as though the presence of small amounts of GO in the PLA matrix in the case of S-2-GO prevent coalescence of the dispersed droplets and therefore made a finer morphology, which is similar to the case of S-2-G.

However, the presence of GO in these two sample was generally insignificant. Thus, some GOs resided in the PMMA phase (which was etched).

In the GO premixed with PLA blend (S-3-GO), the presence of GO in the interface [see Figure 9(b,d)] and in the PLA phase [see Figure 9(a,b)] was observed to conform with the thermodynamics affinity. In fact, some little migration occurred for it to attain equilibrium state.

When GO was premixed with the PMMA and then mixed with PLA (S-4-GO), the dispersed domains became larger in comparison with the other GO filled blends and no GO was observed in the PLA matrix. It seems the GOs settled in the PMMA and could not migrate to the interface as predicted by thermodynamics.

Table IV. The Calculated Wetting Parameter and Filler Localization Prediction

Model system	Grifalco-Good model		Owen-Wendt model		Wu model	
	ω_a	Filler localization	ω_a	Filler localization	ω_a	Filler localization
PLA/PMMA/GNP	4.92	PMMA	2.05	PMMA	1.94	PMMA
PLA/PMMA/GO	6.76	PMMA	−0.08	Interface	−0.14	Interface

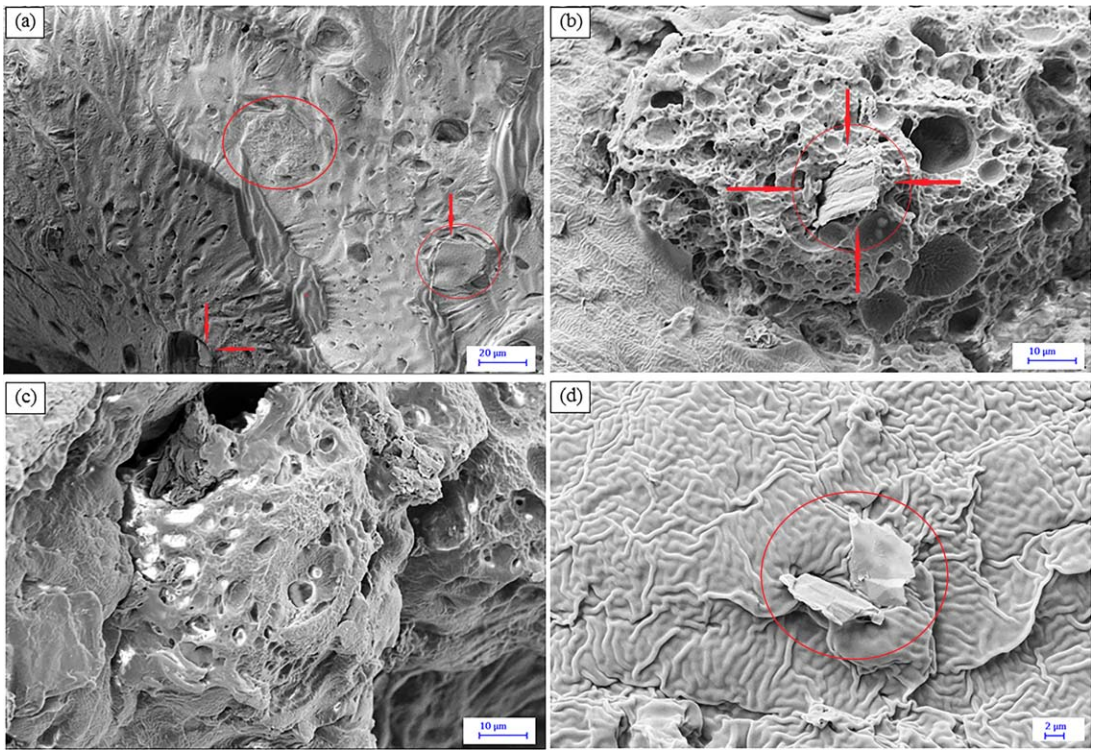

Figure 3. FESEM images of GNP filled PLA/PMMA blends prepared by simultaneous mixing in different magnifications. [Color figure can be viewed in the online issue, which is available at wileyonlinelibrary.com.]

Based on the calculation of Krasovitski and Marmur,[40] this interval of wetting coefficient was strongly narrowed for high aspect ratio fillers. According to their predictions, by increasing the aspect ratio of the filler, the localization of the filler at the interface is improbable, and the filler is located into a better wetting phase even for very small differences in the wettability of the phases.

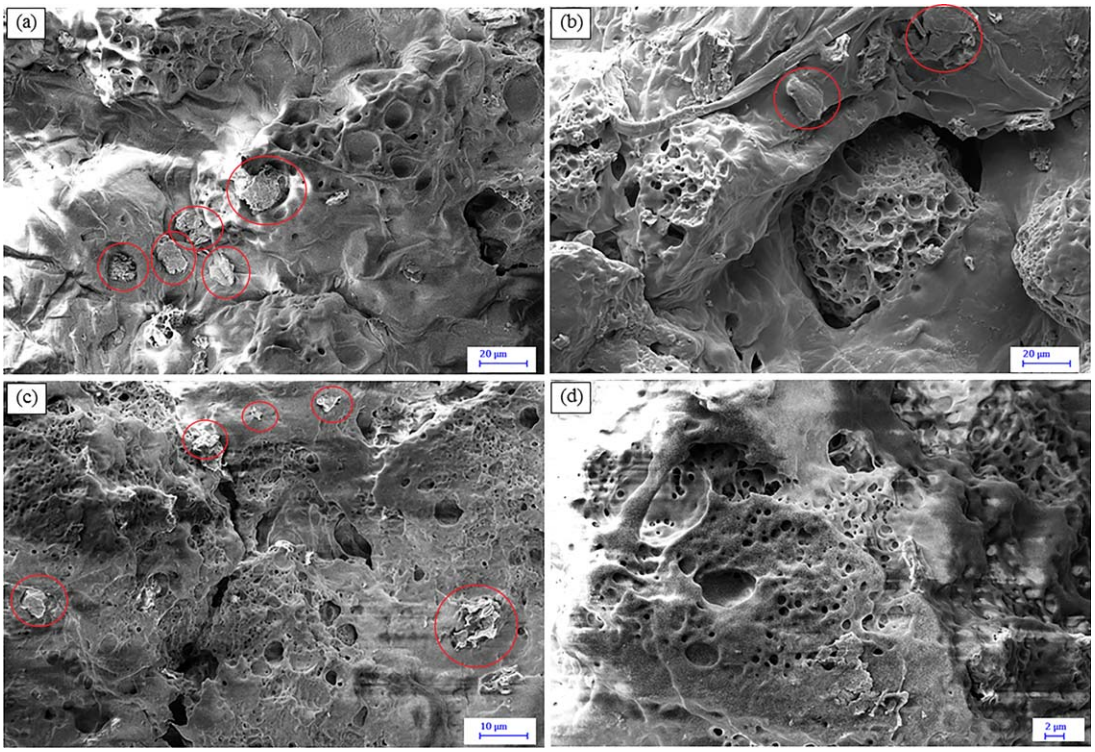

Figure 4. FESEM images of GNP filled PLA/PMMA blends prepared by blend premixed procedure in different magnifications. [Color figure can be viewed in the online issue, which is available at wileyonlinelibrary.com.]

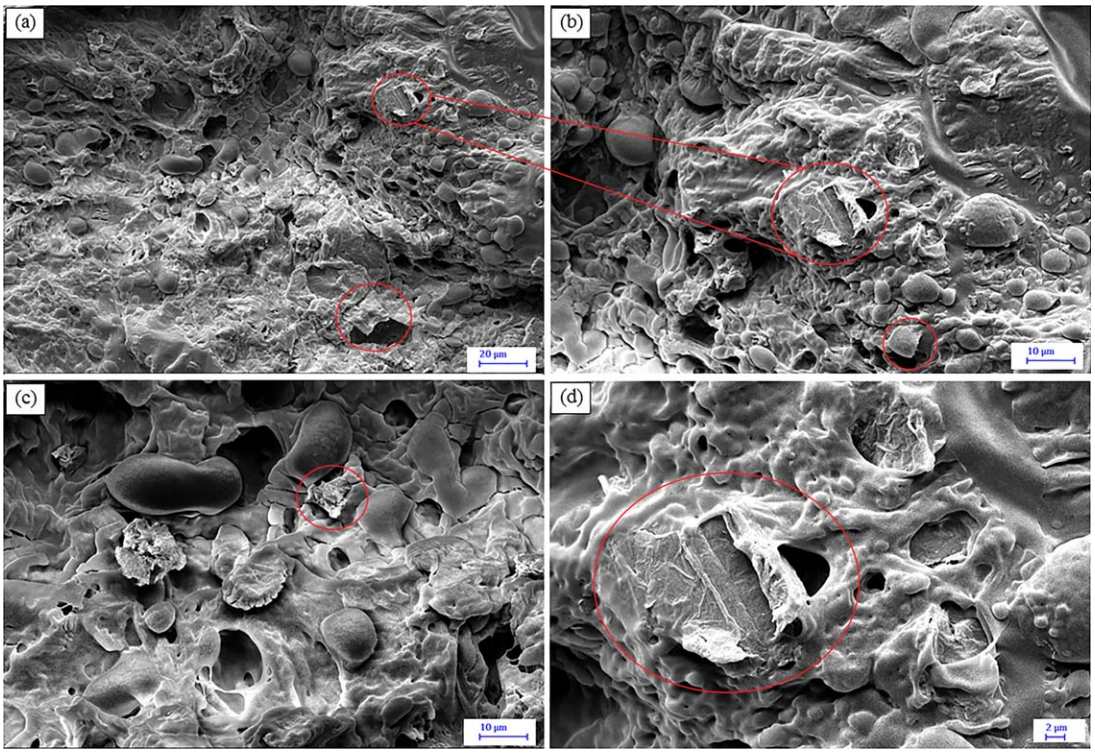

Figure 5. FESEM images of GNP filled PLA/PMMA blends prepared by PLA premixed procedure in different magnifications. [Color figure can be viewed in the online issue, which is available at wileyonlinelibrary.com.]

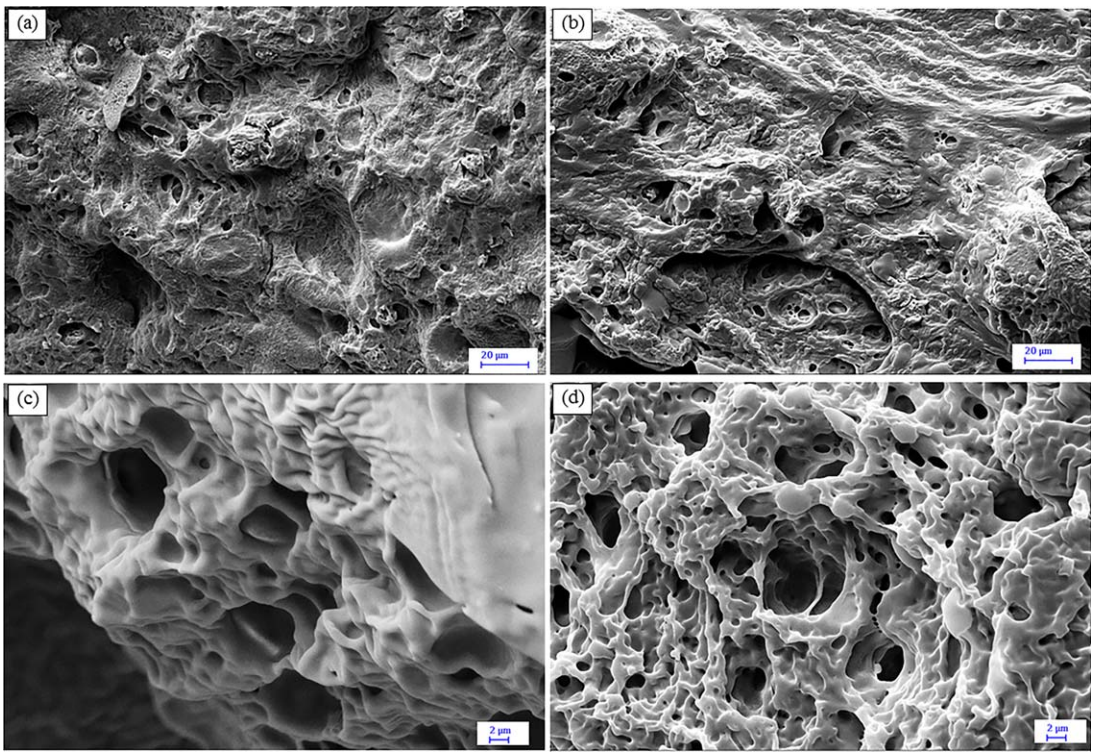

Figure 6. FESEM images of GNP filled PLA/PMMA blends prepared by PMMA premixed procedure in different magnifications. [Color figure can be viewed in the online issue, which is available at wileyonlinelibrary.com.]

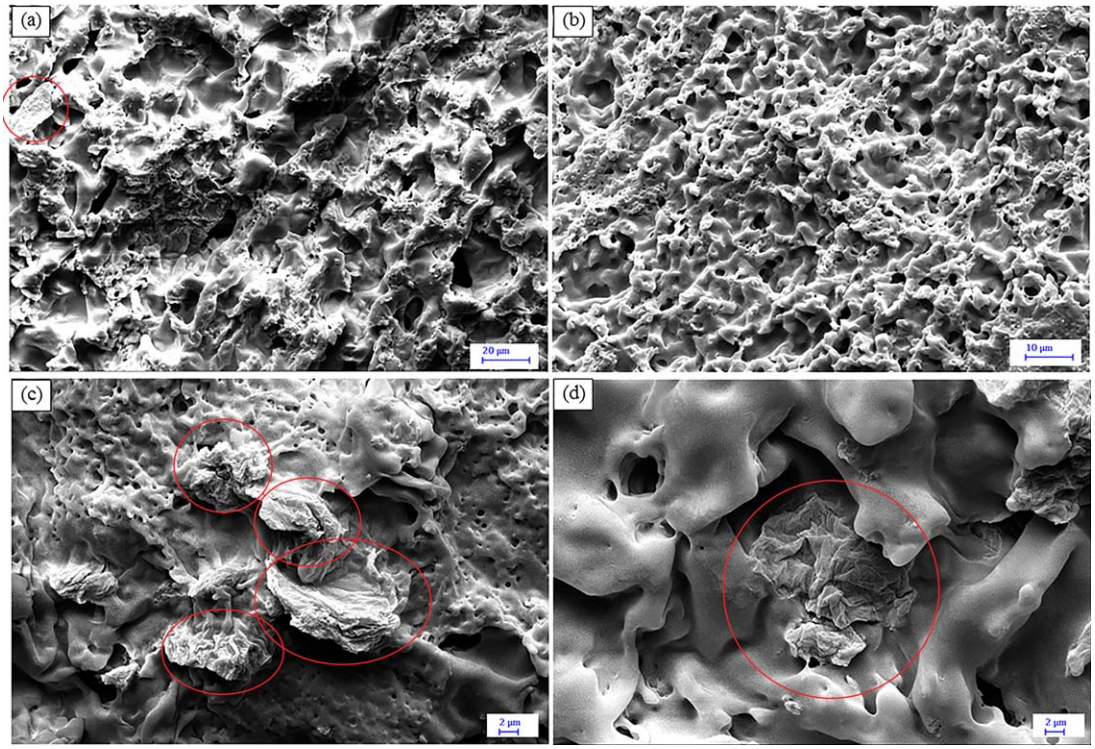

Figure 7. FESEM images of GO filled PLA/PMMA blends prepared by Simultaneous mixing in different magnifications. [Color figure can be viewed in the online issue, which is available at wileyonlinelibrary.com.]

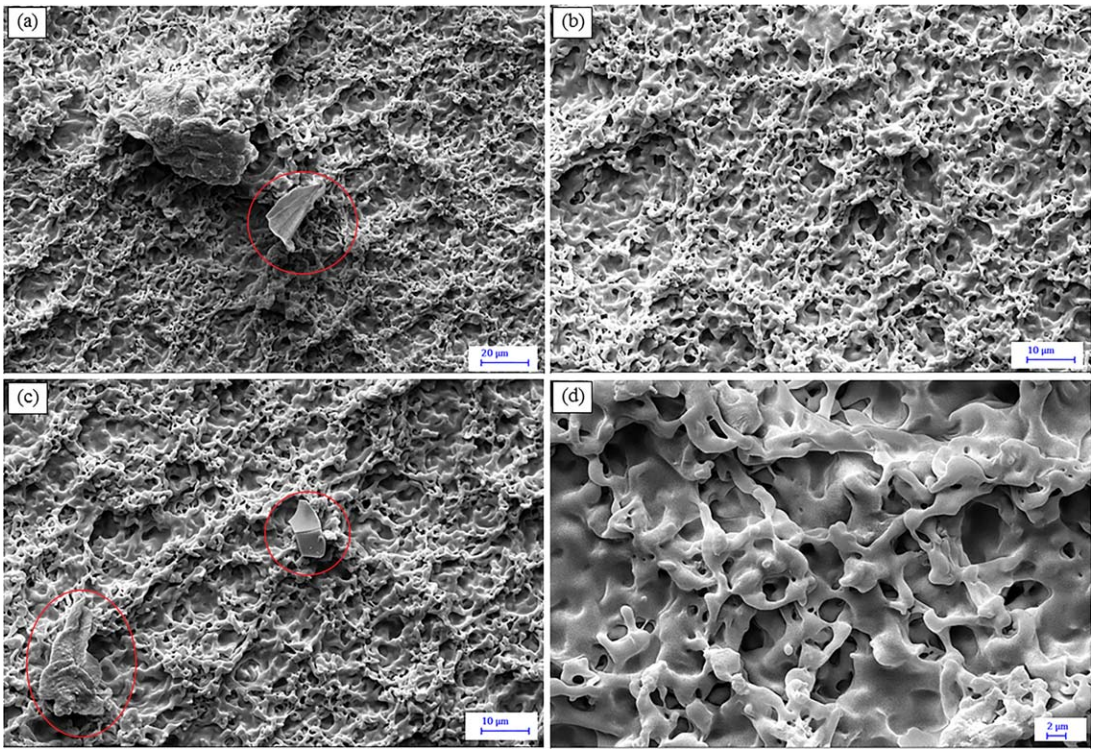

Figure 8. FESEM images of GO filled PLA/PMMA blends prepared by blend premixed procedure in different magnifications. [Color figure can be viewed in the online issue, which is available at wileyonlinelibrary.com.]

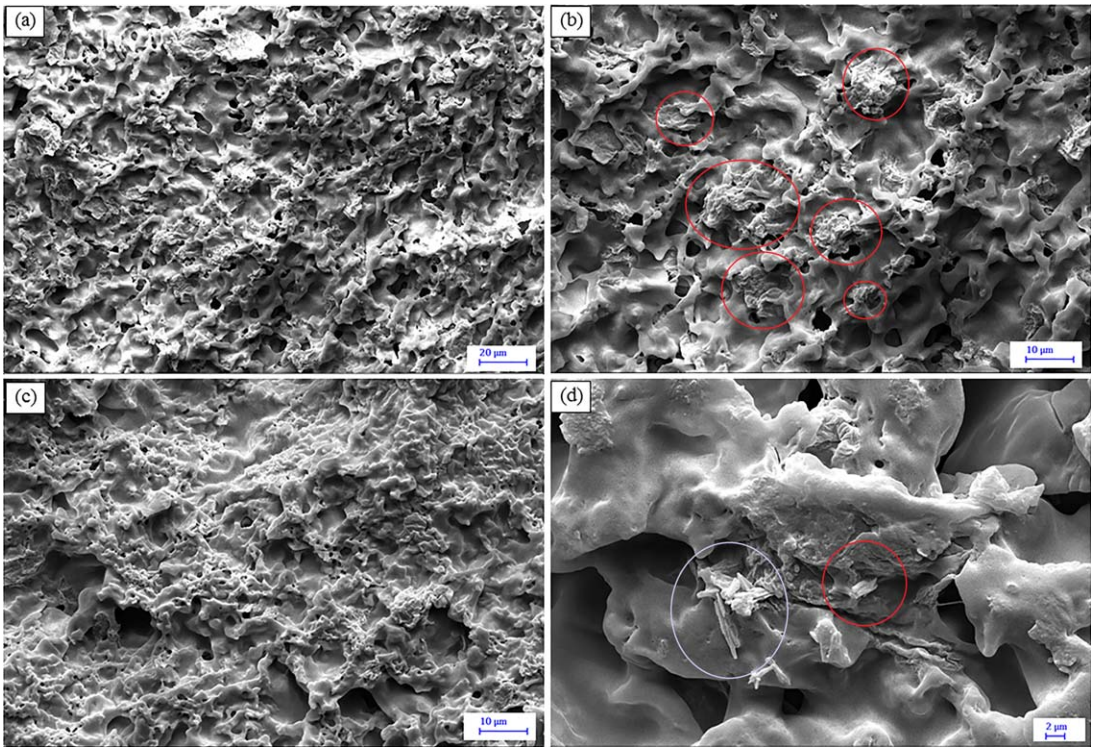

Figure 9. FESEM images of GO filled PLA/PMMA blends prepared by PLA premixed procedure in different magnifications. [Color figure can be viewed in the online issue, which is available at wileyonlinelibrary.com.]

GO has little more interaction with PMMA (as Grifalco-Good predicted) and owing to its high aspect ratio could not migrate to the interface.

Surface Chemistry Dependency of Filler Dispersion and Localization. Morphology comparison of GNP containing blends with GO containing blends indicated that the strong interaction of GO with polymer phases made it to have a lower tendency for migration in order to attain thermodynamic stability. GO localization was mainly dependent on kinetics parameters like mixing sequences; however, GNP tried to attain thermodynamics equilibrium in each processing procedure. The role of thermodynamics was dominant in this case. In addition due to better interaction of GO with polymer phases in comparison with GNP interactions, the dispersion of GO in the blend is better than GNP dispersion so that TEM images showed aggregates of GNP with many layers [Figure 11(a)] while GO exhibited exfoliated structure [Figure 11(b)]. Figure 11 show the TEM images of S-2-GNP and S-2-GO for better comparison between the dispersion and exfoliation of the two graphene based materials.

Rheology Measurement

The rheological behavior of both set of blends at different preparation sequences was also investigated to get more insight about the localization of fillers within the polymer phases of blends.

Figure 12 presents the storage modulus versus frequency of blends containing 0.5, 1 and 3 phr of GNP and GO during different sequences. The shoulder presented on the modulus curves of samples was due to shape relaxation of the PLA phase in the blend.[41,42] The interfacial energies and the interface areas changed periodically during oscillatory shear measurements, but the relaxation time of these changes were much longer than that of the component polymers.[41,43] Thus, an additional shoulder was observed in the G′curves.

For the sample containing 0.5 phr of GNP or GO, no change in the storage modulus behavior of blends was observed. It seems that this small amount of fillers was lower than the rheological percolation threshold and thus the rheological properties almost remained unaffected. Thus, the blends containing 1 and 3 phr nano-fillers were examined. On comparing the storage modulus values of GNP and GO filled blends, it was evident that GNP filled nanocomposites had slightly higher storage modulus.

Basis discussed in literatures,[44–51] the low frequency solid-like behavior of a filled polymer blend indicated that the filler network formation in the matrix and the three dimensional network formed in the dispersed phase cannot make significant changes in the low frequency elastic behavior of the filled blends. Interestingly, from the results shown in Figure 12(a) for the simultaneous mixing process, only the blend containing 3 phr of GNP and GO had filler formed a plateau of low frequencies accompanied by an increase in the storage modulus of several orders of magnitude. These behaviors indicated the onset of the formation of a percolated network and the transition from a viscous liquid to a pseudo-solid like behavior. In the case of blends prepared during the second sequence [Figure 12(b)], the non-terminal behavior at low frequency exhibited at 1 phr loading for both fillers. Thus, it can be concluded that the

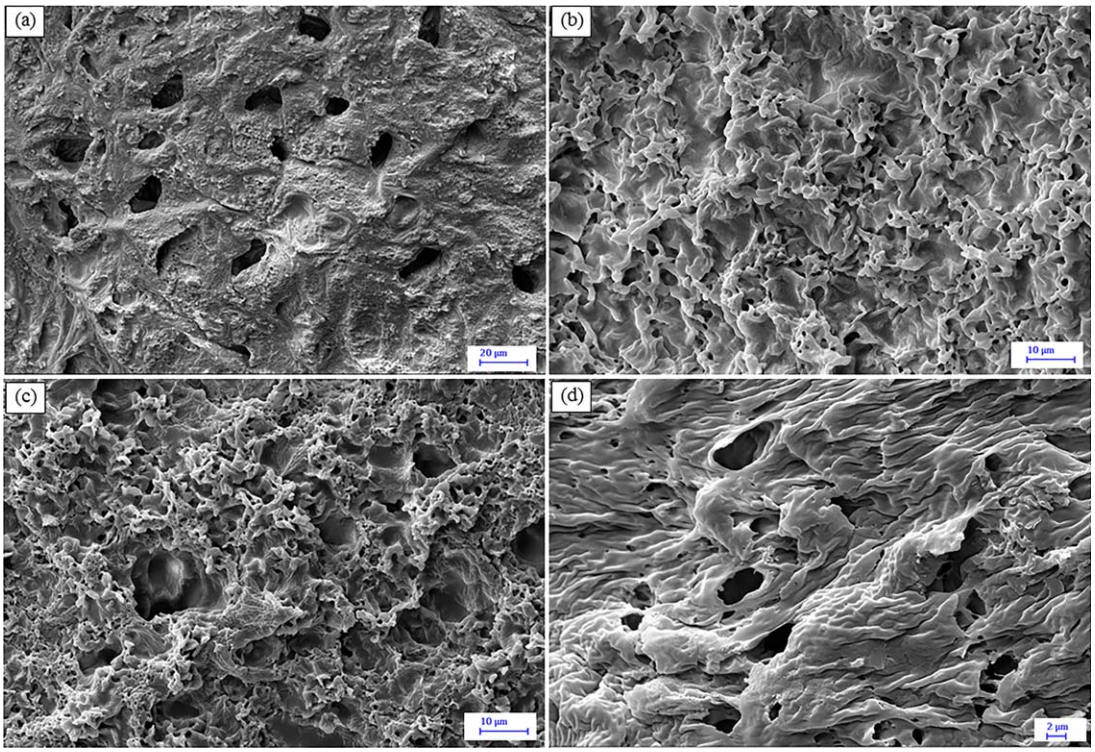

Figure 10. FESEM images of GO filled PLA/PMMA blends prepared by PMMA premixed procedure in different magnifications. [Color figure can be viewed in the online issue, which is available at wileyonlinelibrary.com.]

localization of filler in the matrix during the first sequence (simultaneous mixing) was lower than the blend prepared during the second mixing as proposed from FESEM observations. Figure 12(c,d) exhibit the rheological behavior of blends prepared during the third and fourth sequences, the PLA premixed and PMMA premixed, respectively. When PLA was premixed with nano-fillers, some filler migrated to the PMMA dispersed phase. Thus, it is only when the filler amount rose to 3 phr that the filler network could be formed in the matrix and the non-terminal behavior was observed. In the case of blends premixed with PMMA, no solid-like behavior was observed indicating localization of GNP and GO in the PMMA dispersed phase even at higher loading of filler.

CONCLUSIONS

This study attempts to understand the role of kinetics parameters like mixing sequence in the localization of high aspect ratio fillers. Furthermore, it also attempts to understand how the

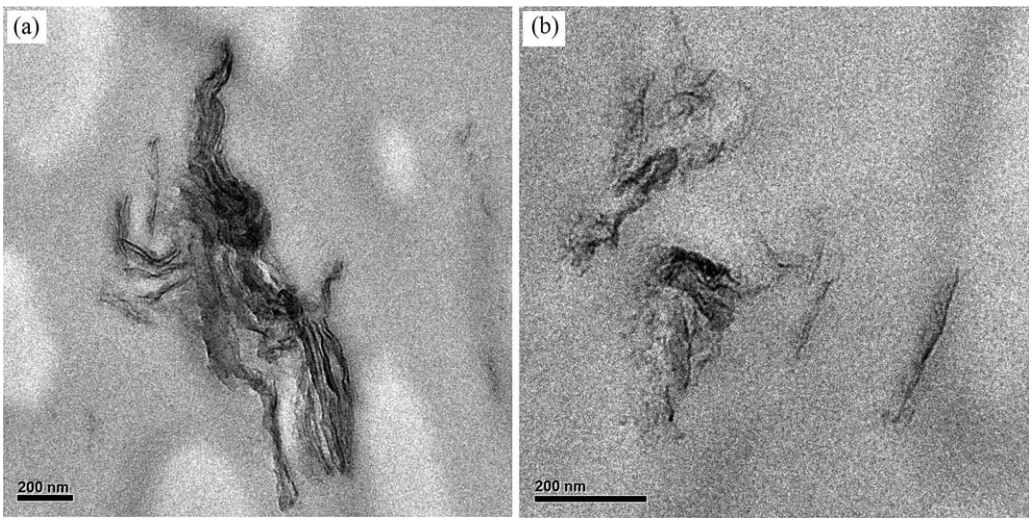

Figure 11. TEM images of dispersion of (a) S-2-GNP and (b) S-2-GO in the PLA/PMMA blends.

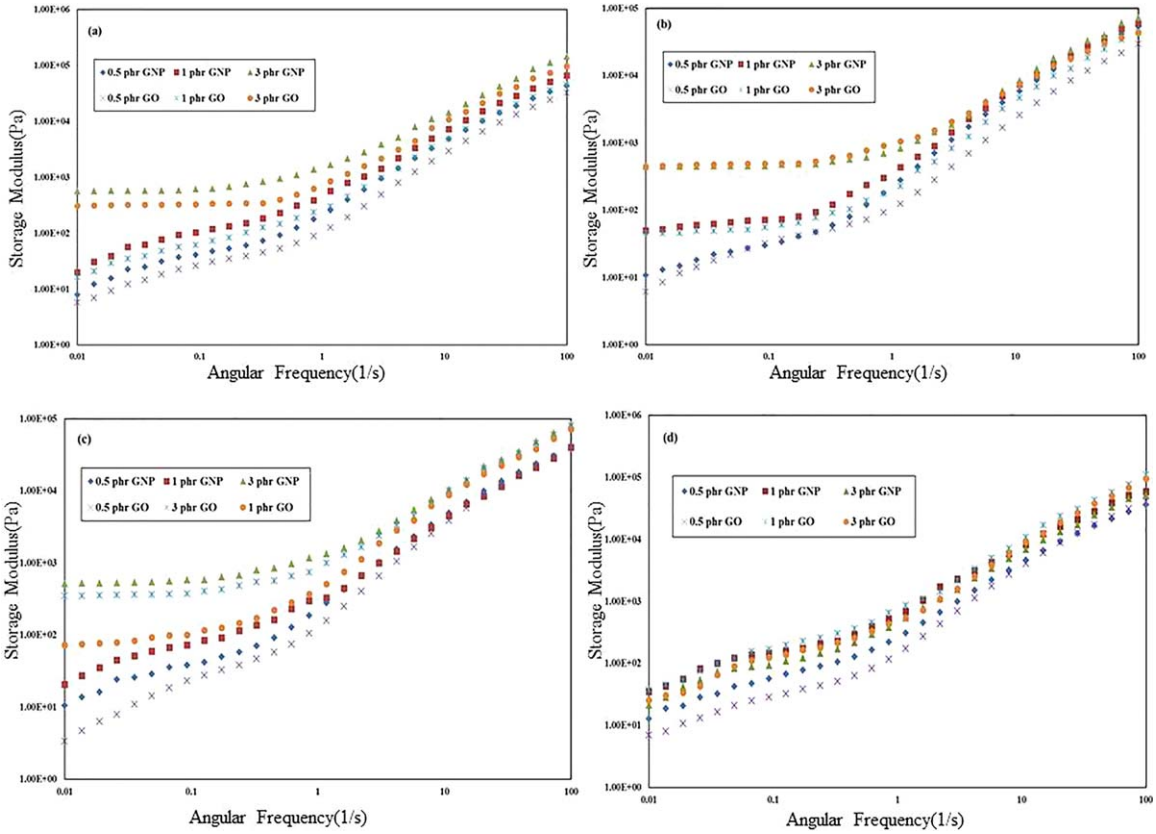

Figure 12. Variation in storage modulus with frequency of GNP and GO filled blends through different sequences: (a) Simultaneous mixing, (b) blend premixed, (c) PLA premixed and (d) PMMA premixed. [Color figure can be viewed in the online issue, which is available at wileyonlinelibrary.com.]

chemical interactions between filler and polymer phases can influence the dispersion and localization of filler. The PLA/PMMA blends filled with GNP or GO were prepared by solution mixing via four different procedures. SEM observations and rheological measurements showed that although from thermodynamic point of view GNP should be placed in PMMA phase, but by varying mixing sequences (as the kinetic changed) it didn't happen surly and it is localized in the other phases too, (PLA phase and interface) and only when mixing sequence was consonant with thermodynamics (forth sequence) the localization of filler was completely confirming the thermodynamic affinity. Even samples are prepared by simultaneous mixing, the thermodynamics didn't have success. It is due to interaction of GNP with both phases.

Localization of GO in the blend was similar to the localization of GNP since didn't conform the thermodynamic, completely. GO must be placed in the interface thermodynamically, but it was in the both phases and tried to settle in the PMMA phase due to a little better wetting in this phase.

Comparison of GNP and GO localization in the blend showed that GOstick more than GNP to the phases that introduce first time, and has lower migration capacity to the its preferred phase.

Thus it can be said that the lower interaction between filler and polymer the easier migration and stronger thermodynamic role was resulted but existence of chemical interaction between filler and polymer phases make the kinetic parameters be dominant in the determination of filler in the polymer blend.

REFERENCES

1. Utracki, L. Polymer Blends Handbook; Kluwer Academic Publishers: Dordrecht, Boston, London, **2002**, p 577.
2. Mittal, V.; Luckachan, G. E.; Matsko, N. B. *Macromol. Chem. Phys.* **2014**, *215*, 255.
3. Dil, E. J.; Favis, B. D. *Polymer* **2015**, *77*, 156.
4. Jin, F. L.; Pang, Q. Q.; Zhang, T. Y.; Park, S. J. *J. Ind. Eng. Chem.* **2015**.
5. Fenouillot, F.; Cassagnau, P.; Majesté, J. C. *Polymer* **2009**, *50*, 1333.
6. Göldel, A.; Kasaliwal, G.; Pötschke, P. *Macromol. Rapid Commun.* **2009**, *30*, 423.
7. José-Yacamán, M.; Miki-Yoshida, M.; Rendon, L.; Santiesteban, J. *Appl. Phys. Lett.* **1993**, *62*, 202.
8. Adamson, A. W.; Gast, A. P. Physical Chemistry of Surfaces, 6th ed.; Wiley: London; New York, **1997**.
9. Ross, S.; Morrison, E. **1988**.
10. Fowkes, F. M. *J. Phys. Chem.* **1963**, *67*, 2538.
11. Owens, D. K.; Wendt, R. *J. Appl. Polym. Sci.* **1969**, *13*, 1741.

12. Cardinaud, R.; McNally, T. *Eur. Polym. J.* **2013**, *49*, 1287.
13. Wu, S. Polymer Interface and Adhesion; M. Dekker, **1982**.
14. Krause, B.; Schneider, C.; Boldt, R.; Weber, M.; Park, H.; Pötschke, P. *Polymer* **2014**, *55*, 3062.
15. Baudouin, A. C.; Bailly, C.; Devaux, J. *Polym. Degrad. Stabil.* **2010**, *95*, 389.
16. Dil, E. J.; Favis, B. D. *Polymer* **2015**, *76*, 295.
17. Elias, L.; Fenouillot, F.; Majesté, J. C.; Martin, G.; Cassagnau, P. *J. Polym. Sci. Part B: Polym. Phys.* **2008**, *46*, 1976.
18. Göldel, A.; Marmur, A.; Kasaliwal, G. R.; Pötschke, P.; Heinrich, G. *Macromolecules* **2011**, *44*, 6094.
19. Göldel, A.; Kasaliwal, G. R.; Pötschke, P.; Heinrich, G. *Polymer* **2012**, *53*, 411.
20. Gubbels, F.; Jérôme, R.; Vanlathem, E.; Deltour, R.; Blacher, S.; Brouers, F. *Chem. Mater.* **1998**, *10*, 1227.
21. Persson, A. L.; Bertilsson, H. *Polymer* **1998**, *39*, 5633.
22. Feng, J.; Chan, C. M.; Li, J. X. *Polym. Eng. Sci.* **2003**, *43*, 1058.
23. Sumita, M.; Sakata, K.; Asai, S.; Miyasaka, K.; Nakagawa, H. *Polym. Bull.* **1991**, *25*, 265.
24. Ibarra-Gómez, R.; Márquez, A.; Ramos-de Valle, L. F.; Rodríguez-Fernández, O. S. *Rubber Chem. Technol.* **2003**, *76*, 969.
25. Chen, G.; Lu, J.; Wu, D. *Mater. Chem. Phys.* **2007**, *104*, 240.
26. Wu, M.; Shaw, L. L. *J. Power Source* **2004**, *136*, 37.
27. Wu, M.; Shaw, L. *J. Appl. Polym. Sci.* **2006**, *99*, 477.
28. Pötschke, P.; Pegel, S.; Claes, M.; Bonduel, D. *Macromol. Rapid Commun.* **2008**, *29*, 244.
29. Liebscher, M.; Blais, M. O.; Pötschke, P.; Heinrich, G. *Polymer* **2013**, *54*, 5875.
30. Childres, I.; Jauregui, L. A.; Park, W.; Cao, H.; Chen, Y. P. *Dev. Photon Mater. Res.* **2013**, *978*.
31. Ferrari, A. C.; Basko, D. M. *Nat. Nanotechnol.* **2013**, *8*, 235.
32. Katada, A.; Buys, Y. F.; Tominaga, Y.; Asai, S.; Sumita, M. *Colloid Polym. Sci.* **2005**, *284*, 134.
33. Wu, S. In The Wiley Database of Polymer Properties; John Wiley & Sons, Inc., **2003**.
34. Falsafi, A.; Mangipudi, S.; Owen, M. J. In Physical Properties of Polymers Handbook; Springer, **2007**.
35. Wang, S.; Zhang, Y.; Abidi, N.; Cabrales, L. *Langmuir* **2009**, *25*, 11078.
36. Woltornist, S. J.; Oyer, A. J.; Carrillo, J. M. Y.; Dobrynin, A. V.; Adamson, D. H. *ACS Nano* **2013**, *7*, 7062.
37. Perez-Mendoza, M.; Almazan-Almazan, M.; Mendez-Linan, L.; Domingo-García, M.; López-Garzón, F. *J. Chromatogr. A* **2008**, *1214*, 121.
38. Paydayesh, A.; Azar, A. A.; Arani, A. J. *J. Macromol. Sci., Part B* **2015**, *00*,
39. Paydayesh, A.; Azar, A. A.; Arani, A. J. *Ciencia & Natura* **2015**, *37*, 15.
40. Krasovitski, B.; Marmur, A. *J. Adhes.* **2005**, *81*, 869.
41. Wu, D.; Zhang, Y.; Zhang, M.; Yu, W. *Biomacromolecules* **2009**, *10*, 417.
42. Lee, H. M.; Park, O. O. *J. Rheol. (1978-Present)* **1994**, *38*, 1405.
43. Yu, W.; Bousmina, M.; Grmela, M.; Zhou, C. *J. Rheol. (1978-Present)* **2002**, *46*, 1401.
44. Du, F.; Scogna, R. C.; Zhou, W.; Brand, S.; Fischer, J. E.; Winey, K. I. *Macromolecules* **2004**, *37*, 9048.
45. Pötschke, P.; Fornes, T.; Paul, D. *Polymer* **2002**, *43*, 3247.
46. Pötschke, P.; Abdel-Goad, M.; Alig, I.; Dudkin, S.; Lellinger, D. *Polymer* **2004**, *45*, 8863.
47. Nogales, A.; Broza, G.; Roslaniec, Z.; Schulte, K.; Šics, I.; Hsiao, B. S.; Sanz, A.; García-Gutiérrez, M. C.; Rueda, D. R.; Domingo, C. *Macromolecules* **2004**, *37*, 7669.
48. Hu, G.; Zhao, C.; Zhang, S.; Yang, M.; Wang, Z. *Polymer* **2006**, *47*, 480.
49. Wu, D.; Wu, L.; Zhang, M. *J. Polym. Sci. Part B: Polym. Phys.* **2007**, *45*, 2239.
50. Wu, D.; Wu, L.; Sun, Y.; Zhang, M. *J. Polym. Sci. Part B: Polym. Phys. 45*, 3137. **2007**,
51. Wu, D.; Wu, L.; Zhang, M.; Zhao, Y. *Polym. Degrad. Stabil. 93*, 1577. **2008**,